AIAA 81-0376R

Atmospheric Ammonia: Measurements and Modeling

James M. Hoell Jr.* and Joel S. Levine*
NASA Langley Research Center, Hampton, Va.
and
Tommy R. Augustsson† and Charles N. Harward‡
Old Dominion University, Norfolk, Va.

Ammonia is a unique constituent of the terrestrial atmosphere in that it is the only gaseous base. Ammonia readily forms aerosols and, by virtue of its high solubility, controls the pH of cloud droplets and precipitation. Over the past year a ground-based solar viewing infrared heterodyne radiometer has been used at Langley Research Center to infer the vertical distribution of ammonia. Ground level in situ measurements of ammonia have also been obtained to supplement the profile data. The ammonia profiles have been analyzed and interpreted with a one-dimensional photochemical model of the troposphere to assess the sources and sinks of NH_3.

Introduction

AMMONIA (NH_3) is a key gas in the troposphere, yet it is one of the most poorly understood and one of the most difficult to measure.[1,2] Ammonia is the only gaseous base constituent of the atmosphere, an environment of acid constituents, e.g., sulfuric acid (H_2SO_4) and nitric acid (HNO_3) which result from the oxidation of several anthropogenic gases, e.g., sulfur dioxide (SO_2) and nitrogen dioxide (NO_2), respectively. By virtue of its high solubility, NH_3 controls the pH of cloud droplets and the acidity of rain and snow. Ammonia may also play a significant role in determining the rate of conversion of gaseous sulfur dioxide to sulfate aerosols since it controls the acidity of the system.[3] Ammonia readily reacts with gaseous nitric acid and sulfuric acid to form ammonium nitrate (NH_4NO_3) and ammonium sulfate [$(NH_4)_2SO_4$] aerosols. Preliminary epidemiological studies suggest that ammonia-containing aerosols may have adverse effects on health. In addition, ammonium aerosols may modify the radiative budget of our planet, and NH_3 itself may affect climate due to its absorption in the thermal infrared around 10 μm, the middle of the atmospheric window.[4] Ammonia has been suggested as a significant source of stratospheric nitrogen oxides (NO_x).[5] Stratospheric NO_x controls the levels of ozone in the stratosphere, which shields the surface from deadly solar ultraviolet radiation.

While there are fundamental deficiencies in our understanding of the sources and sinks of NH_3, it does appear that NH_3 is biological in origin with the Earth's surface the primary source of NH_3, with different processes controlling the production of NH_3 in different regions. In England, urine from domestic animals may be the dominant source of NH_3.[6] Volatilization of NH_3 from undisturbed (nonfertilized) land[1] and from fertilized agricultural fields[7,8] are additional sources of ammonia. Thermodynamic equilibrium calculations indicate that the atmospheric equilibrium mixing ratio of NH_3 should be about 10^{-35}.[9] The measured atmospheric mixing ratio of about 1×10^{-9}, a 26 order of magnitude enhancement over the theoretical equilibrium mixing ratio, is a testimonial to the ability of micro-organisms to maintain drastic disequilibrium conditions in the chemistry of natural systems. In addition to the volatilization of man-made nitrogen agricultural fertilizer, other anthropogenic sources of NH_3 may be industrial activity[10] and coal conversion and combustion processes.[6,11] In the future, the production of NH_3 from anthropogenic activities may significantly increase, as the use of nitrogen agricultural fertilizer continues its exponential worldwide increase and as we switch to greater dependence on coal.

Most of our early knowledge concerning the concentration of tropospheric NH_3 is due to in situ measurements of Georgii and Muller.[12] These measurements indicate that NH_3 exhibits great temporal and spatial variability. Georgii and Muller[12] found that the ground concentration of NH_3 was about a factor of 3 higher on warm days than on cool days. In addition, they found that the concentration of NH_3 decreased rapidly with altitude, reaching a constant background concentration at an altitude of about 1.5 km on winter days and at about 3 km on warm days.

The purpose of this paper is to discuss results from a program designed to study the factors controlling the production and vertical distribution of NH_3. This study, initiated in March 1979, is being conducted at the NASA Langley Research Center using a solar viewing Infrared Heterodyne Radiometer (IHR) and two in situ ammonia sampling instruments. Vertical profiles of atmospheric ammonia have been inferred from the spectrally resolved solar absorption data obtained using the IHR. The in situ measurements have been obtained from ground-based sites to supplement the IHR data and to extend our measurement capability to periods of cloud cover (which precludes the use of the IHR) and to conditions which produce ammonia levels below the sensitivity of the IHR (less than 0.5 ppbv). Results from our measurements show a seasonal variation in ammonia with minimum NH_3 levels in the winter months and maximum NH_3 levels in the spring. Results over two years also suggest that the seasonal background concentration is strongly dependent upon meteorological conditions. Interpretation of our results with respect to the factors that control the surface concentration and the vertical distribution of ammonia is also discussed.

Instrumentation

The Infrared Heterodyne Radiometer

The high spectral resolution available from optical heterodyne instruments is typically achieved through the use of one or more narrow bandpass intermediate frequency (IF) filters. These filters are generally selected to coincide with particular portions of the infrared (IR) spectrum that have been shifted by the heterodyne process into the microwave frequency region. This is illustrated in Fig. 1a where a synthetic atmospheric spectrum of the $aQ(6,6)$ ammonia line is

Presented as Paper 81-0376 at the AIAA 19th Aerospace Sciences Meeting, St. Louis, Mo., Jan. 12-15, 1981; submitted March 6, 1981; revision received July 23, 1981. This paper is declared a work of the U. S. Government and therefore is in the public domain.

*Senior Research Scientist.
†Visiting Scientist.
‡Assistant Research Professor.

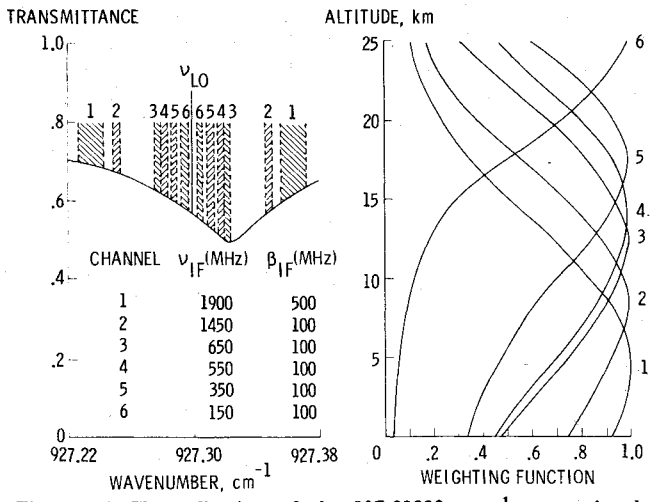

Fig. 1 a) Channelization of the 927.32323 cm^{-1} ammonia absorption line and b) weighting functions corresponding to each IF channel.

shown along with the relative position of the laser local oscillator (LO) and six IF channels. Note that because of the image property of heterodyne radiometers, the output from each IF channel is the sum of the radiation over the spectral regions $(\bar{\nu}_{LO}-\nu_{IF}/c\pm\beta_{IF}/2c)$ and $(\bar{\nu}_{LO}+\nu_{IF}/c\pm\beta_{IF}/2c)$ where $\bar{\nu}_{LO}$ is the LO wave number, ν_{IF} the center frequency of the IF filter, and β_{IF} the IF filter bandpass. Thus, analysis of data from a heterodyne radiometer must account for radiation from both of these sidebands.

The ammonia profiles reported here were obtained from solar absorption measurements at the six IF channels shown in Fig. 1a along with a seventh channel (described below) which provided a normalizing reference signal. The average solar radiance I_j detected in the jth IF channel can be expressed as

$$I_j = I_j^\circ \tau_{jc} \tau_{jg} \tag{1}$$

where I_j° is the unattenuated solar radiance, τ_{jc} the atmospheric continuum transmittance related to molecular (i.e., water vapor) and aerosol absorption and scattering, and τ_{jg} the noncontinuum molecular transmittance. Note that each parameter identified in Eq. (1) is considered to be averaged over the upper and lower sideband of the given channel. Normalization of the solar radiance detected in each IF channel by that observed in the reference channel is required to minimize errors associated with the continuum interference effects τ_{jc} and the fluctuations in the source intensity I_j°. Accordingly, the desired quantity is the atmospheric transmission ratio given by

$$R_j = \tau_{jg}/\tau_g^{ref} \tag{2}$$

where τ_g^{ref} is the atmospheric transmissivity due to molecular line absorption at the reference channel wavelength. Equation (2) is obtained from Eq. (1) only if the source radiation and atmospheric continuum transmittance are equal at the wavelengths for the reference and jth signal channel.

The IHR provides for a reference and the six signal channels through the use of two $^{13}C^{16}O_2$ laser LOs. The reference and signal LO are the $R(8)$ transition at 920.2194 cm^{-1} and $R(18)$ transition at 927.3004 cm^{-1}, respectively. Effects on the measured R_j due to the more abundant isotope of CO_2 are minimized by using $^{13}C^{16}O_2$ LOs; and for these LO transitions, the contribution to R_j due to the combined effects of water vapor continuum,[13] solar radiation, and contributions due to atmospheric $^{13}C^{16}O_2$ is negligible. Moreover, analysis of lower resolution atmospheric absorption spectral[14] and synthetic spectral calculated using available molecular line parameters from McClatchey et al.[15] indicates that contributions to Eq. (2) from other interfering species is also negligible.

Vertical profiles of ammonia are inferred from a set of R_j's measured simultaneously at different positions on an absorption feature. Collisional broadening of the absorption feature providing the mechanism by which the spectrally resolved transmission ratios are coupled to an altitude region. The altitude dependence of the absorption coefficient for each channel serves as the weighting function and a plot of altitude vs the normalized absorption coefficient for a given IF channel (Fig. 1b) indicates the vertical sensitivity that can be obtained. The upper altitude limit available from this technique is governed by the decrease in the collisional broadening effects as the pressure decreases with altitude. For ammonia, the upper limit is around 30 km where the collisional and Doppler broadened half widths are approximately equal.

The density profile $\rho(z)$ is inferred from R_j through the use of an iterative inversion technique with successive approximations to $\rho(z)$ at altitude z given by[16]

$$\rho^{k+1}(z) = \rho^k(z)\left\{\sum_j K_j^*(z)\ln R_j/\ln R_j^k\right\}\Big/\sum_j K_j^*(z) \tag{3}$$

where K_j^* is the normalized absorption coefficient for ammonia averaged over channel j, and R_j and R_j^k are the measured and the kth approximation to the normalized transmission ratio, respectively. The inversion process starts with an initial ammonia profile $\rho^\circ(z)$. The transmission ratio R_j° is calculated and compared with the measured R_j. If the rms difference between R_j^k and R_j is greater than the system noise, a new approximation to $\rho(z)$ is calculated using Eq. (3).

For each iteration on $\rho^k(z)$, the calculated R_j^k is obtained using a line-by-line computer model for all transmittance and absorption calculations. This model considers both Lorentz and Voigt line shapes and includes temperature and pressure effects on spectral line strengths and half widths. With the exception of the single ammonia line observed here, line parameter data for the inversion algorithm were obtained from McClatchey.[15] The data for the observed ammonia line are given as: line center = 927.32323 cm^{-1},[17] line strength = 4.09×10^{-19} cm^{-1}/(molecule cm^2),[15] foreign gas broadened half width = 0.08 cm^{-1}/atm.[18] The atmospheric model in the inversion algorithm includes H_2O, CO_2, and NH_3 profiles along with a pressure and temperature profile. The H_2O, pressure, and temperature profiles were obtained from the U. S. Standard Atmosphere Supplements, 1962, for 30° N latitude and the appropriate climatological period. Little error is expected from the use of a standard H_2O profile since the reference channel provides near cancellation of water vapor effects on the transmission ratio. Further, the small lower state energy of the ammonia transition used here (i.e., $E''=283.276$ cm^{-1})[15] coupled to the temperature dependence of the Lorentzian half width and the rotational partition function minimizes errors associated with the temperature profile. The analysis reported by Seals and Peyton[16] concludes that temperature profile bias errors as large as ±5 K introduce inversion errors of less than ±0.25 ppbv.

The IHR, described in detail by Peyton et al.[19] is shown schematically in Fig. 2. The optical package consists of two Dicke-switched radiometer sections which share a common input lens, reference blackbody source, and calibration source. The solar radiance is collected using a 2 in. diam (f/6.5) zinc selinide lens which focuses the incoming radiance onto two high-speed photovoltaic HgCdTe photomixers (provided by D. L. Spears, MIT Lincoln Laboratories). These two photomixers and their corresponding CO_2 laser LOs provide the reference and ammonia absorption channels. A long pass optical filter, which cuts in at 8 μm, limits the amount of solar radiance reaching the photomixers. The infrared Dicke switch alternately switches the field of view of each photomixer between the solar radiance and the reference

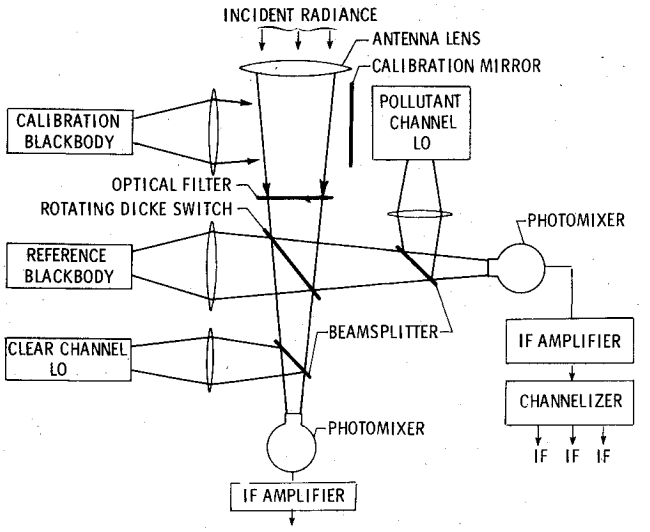

Fig. 2 Schematic of the Infrared Heterodyne Radiometer (IHR).

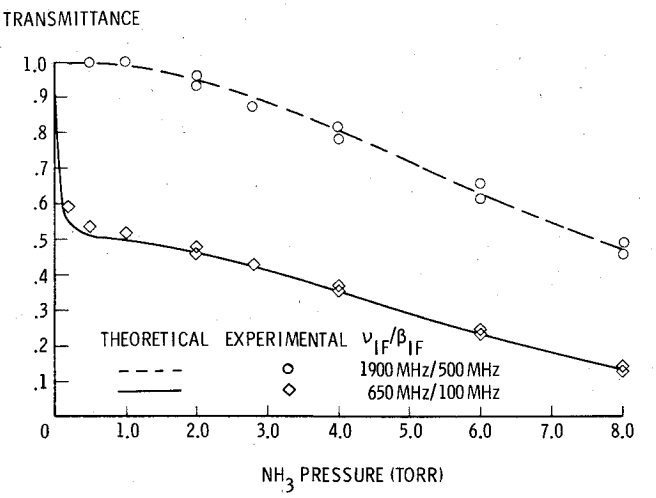

Fig. 3 Comparison of the theoretical and experimental transmittance of an ammonia cell 10 cm in length.

blackbody. Approximately 10% of the radiation from each LO is directed onto its respective photomixer. During alternate half cycles of the Dicke switch, radiation from the sun or reference blackbody is combined with the LO radiation via the beamsplitter. The calibration mirror is used to insert a variable 300-1300 K calibration blackbody into the optical path.

The radio frequency (RF) heterodyne signal from the photomixer monitoring attenuation due to atmospheric ammonia is amplified using a broadband (5 MHz to 2 GHz) IF amplifier and then power split into six channels. Each channel contains a preselected IF filter, RF square-law detector, and a lock-in amplifier referenced to the Dicke-switch frequency. With the exception of the power splitter, a similar train of electronics is used in the reference channel. The IF filters utilized here were selected to maximize the SNR while providing an optimum distribution of weighting functions. They were centered at 150, 550, 650, 1450, and 1900 MHz from the $R(18)$ LO, and 55 MHz from the $R(8)$ reference LO. The 1900 MHz channel, located on the wing of the NH_3 feature, had a bandwidth of 500 MHz; all the remaining channels had a 100 MHz bandwidth.

During the measurement program, routine checks on the performance of the IHR were conducted using a variable temperature (300-1300 K) blackbody to verify the linearity and determine the response of the IHR. A complete calibration (i.e., 6-10 temperature settings) was normally conducted each day with a repeat of the high (1300 K) and low points (300 K) before and after each data run. Measurements were also performed to verify the accuracy of the ammonia line parameters used in the inversion algorithm by comparing the measured and calculated transmissivity of a cell containing pure ammonia and ammonia broadened by an atmosphere of nitrogen. These transmissivity measurements were obtained using the IHR and a 1300 K blackbody source. Agreement between the measured and the calculated pressure broadened transmissivity using the ammonia parameters noted above was about 4%. It is felt that the major source of error for these measurements was due to uncertainties in determining the pressure of ammonia after introduction of nitrogen into the absorption cell. Figure 3 shows a similar set of measurements for a wider range of optical depths obtained by using pure ammonia. The comparison between the measured and calculated transmissivity is shown for the IF channel near the ammonia line center (i.e., $\nu_{IF} = 650$ MHz) and the wing channel ($\nu_{IF} = 1900$ MHz). Note that since pure ammonia was used, a self-broadening half width of 0.63 cm^{-1}/atm has been used in the calculations.[15] A similar set of results were obtained when using the sun as a source after removing atmospheric effects. As a final check on the IHR data a series of simultaneous IHR and aircraft in situ ammonia measurements were conducted in June 1979.[20] Teflon packed in situ sampling tubes (described below) were mounted on a Cessna 402 and air samples collected at altitudes of 1.6 and 3 km. The inferred profiles from the IHR and the in situ data indicated ammonia levels in the 1-2 ppbv range, with the in situ data points generally contained within the uncertainty envelope of the IHR profiles. These coordinated measurements represent the first validation of the ability of the IHR to measure atmospheric ammonia remotely.

In Situ Monitors

Ground level in situ measurements of ammonia were performed using two sampling techniques to preconcentrate ambient ammonia and a photoacoustic cell for quantitative analysis of the collected ammonia. Both sampling configurations were developed and field tested under EPA programs.[21,22] With both sampling systems, collection and preconcentration of ammonia are accomplished by drawing ambient air through a collection tube containing a medium that preferentially adsorbs ammonia. The amount of ammonia collected is proportional to the sample flow rate, the efficiency of collection, the collection time, and the ammonia concentration.

In one system, the air sample passes first through a Teflon prefilter to eliminate particulate interference and then through a quartz tube containing Teflon beads (i.e., Chromosorb T). Studies by McClenney and Bennett[21] have shown that the Teflon-packed tubes selectively adsorb ammonia with a collection efficiency greater than 95%. The ammonia loading, however, is limited to 60 ng and the collection times must be less than 40 min. Additional studies by Harward et al.[23] have shown that care must be exercised in using the particulate filters since ammonia can be released or removed by the filter material depending upon its prior exposure to ammonia. Results reported by Harward et al.[23] indicate that an equilibrium condition must be established on the filter material to avoid contamination of the air sample. Accordingly, for all data reported here, ambient air was routinely drawn through the filter for approximately 20 min prior to installing the Teflon-packed collection tube in the collection system. Sampling times with the collection tube in place typically ranged 15-30 min with a flow rate of 1 l/min.

The second type of collection tube used during the latter portion of the measurements reported here consists of a hollow quartz rod coated on its interior with WO_3 which acts as the adsorbing medium for ammonia. The advantage of this type of tube over the Teflon-packed tube is twofold. First,

with the proper combination of tube length and flow rate,[22] few, if any, particulates are collected, thereby eliminating the need for the particulate filter upstream of the collection tube. Second, the release time of the adsorbed ammonia is decreased by approximately an order of magnitude, thereby increasing the preconcentration factor. This results in an increase in sensitivity or, conversely, a decrease in the sampling time.

Desorption of ammonia collected on both types of collection tubes is accomplished by heating the tube. Since the ammonia is released over a time interval which is short compared to the collection time, preconcentration of ammonia occurs. The ratio of the collection time to release time (i.e., preconcentration factor) is typically 15-20 for the Teflon-packed tubes, and 150-200 for the WO_3-coated tubes.

Quantitative analysis of the adsorbed ammonia from either type of collection tube was performed using a photoacoustic cell with a Helmholtz resonator[24] and a CO_2 laser. The desorbed ammonia was carried into the photoacoustic cell using a continuous flow of helium through the collection tube during the heating cycle. Since the photoacoustic technique detects ammonia directly via absorption of CO_2 radiation tuned to an ammonia absorption feature, interfering effects from other species which may also be adsorbed during the collection process are minimized. Studies by McClenny and Bennett[21] comparing detection of the desorbed gas via chemiluminescence and photoacoustic detection and by Harward et al.[23] comparing photoacoustic detection using $^{13}C^{16}O_2$ and $^{12}C^{16}O_2$ laser transitions substantiate the high degree of specificity for the collection and detection system. Moreover, comparison studies conducted at the Langley Research Center show good agreement between the two collection techniques.[23] During our studies both the $R(18)$ $^{13}C^{16}O_2$ transition at 927.3004 cm^{-1} and the $R(30)$ $^{12}C^{16}O_2$ transition at 1084.6352 cm^{-1} have been used for analysis of collected samples.

Calibration of the collection and photoacoustic system was performed using a triple-dilution system similar to that described by Baumgardner[25] to establish a known concentration of ammonia in a flow of clean humidified air. The amount of ammonia injected into the airstream was based on the permeation of ammonia through Teflon tubing with the permeation rate being determined by periodic measurements of the weight loss from the tube. By maintaining the permeation tube at a constant temperature and a constant flow rate throughout the dilution and collection system, various nanogram loadings of ammonia were obtained simply by varying the sampling time from the dilution manifold. The integrated response from the photoacoustic system is linearly proportional to the amount of ammonia collected. Calibration of the overall in situ system was conducted throughout the measurement program for both types of collection tubes. For the Teflon-packed collection tubes the reproducibility associated with each calibration point was approximately 20%, with a laser power on the order of 1 W. For the WO_3-coated tubes the reproducibility was approximately 5% for the same laser power. The minimum detectable concentration for the Teflon collection tubes is ~0.25 ppbv, and for the WO_3 system it is less than 0.08 ppbv.

Measurements

The measurement program reported here began at Langley Research Center during the latter part of March 1979. The initial measurements, performed with the IHR, were supplemented with ground level in situ measurements beginning in August 1979. The IHR was located in a laboratory area with a 20 cm heliostat on the roof to track and direct solar radiation into the laboratory. Throughout the year the solar viewing angle was generally limited to about 80 deg from the zenith for both sunrise and sunset. Results from both the IHR and in situ measurements illustrating the seasonal variability in atmospheric ammonia observed from March 1979 through

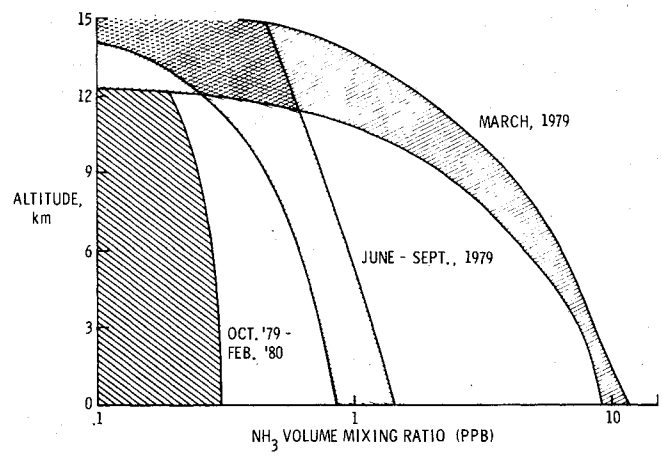

Fig. 4 Seasonal variation of the vertical distribution of atmospheric ammonia.

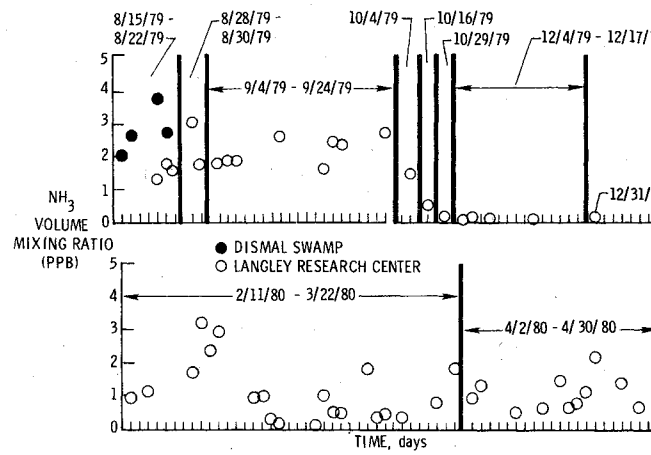

Fig. 5 Seasonal variation of ground level ammonia.

April 1980 are shown in Figs. 4 and 5. The shaded areas shown in Fig. 4 contain approximately 90% of the profiles that were obtained during the indicated time period. The shaded area at the far left of this figure represents the sensitivity limits of the current IHR. Each profile contained within the shaded area was inferred from four sets of the transmission ratios, R_j, measured over approximately 1 h. For each set of data, two initial profiles—one a constant 25 ppbv and the other a constant 0.3 ppbv—were used to initiate the inversion algorithm. In general, the difference between the profiles resulting from each initial guess was less than 0.05 ppbv at all altitudes. For each inversion profile, the rms residual between the calculated and measured transmission ratios was less than 0.01. The profiles for the four sets of R_j are grouped together and make up a single profile envelope (e.g. shown as dashed curve in Figs. 9 and 10). The width of this envelope is taken to be the uncertainty for an individual profile. Each in situ data point shown in Fig. 5 represents the average of three to six 30 min samples taken throughout a normal 8 h work day.

The summer to winter seasonal variations suggested by the results shown in Figs. 4 and 5 are similar to those reported by Georgii and Muller,[12] namely, a significant drop in the ammonia concentration from summer to winter. This type of seasonal decrease is not entirely unexpected since the major source of ammonia is believed to originate from biological sources which are less active during winter. Of particular interest, however, are the relatively high levels of ammonia observed during the latter part of March 1979 (Fig. 4). This trend of high levels (~10 ppbv at the surface) followed by a decrease to lower relatively constant levels in the summer time period, is similar to that reported by Peyton et al.[19] Peyton's

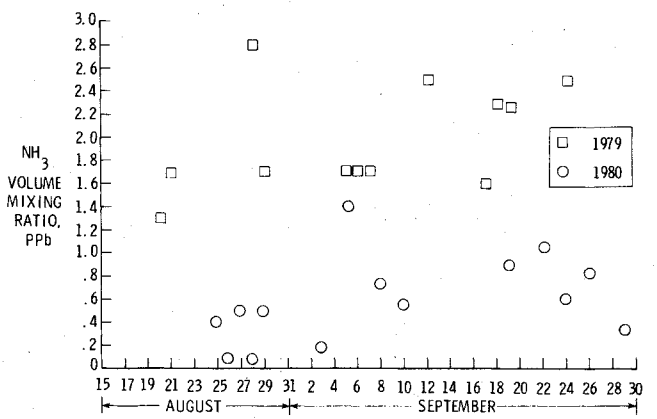

Fig. 6 Ground level in situ measurements of ammonia obtained at Langley Research Center during 1979 and 1980.

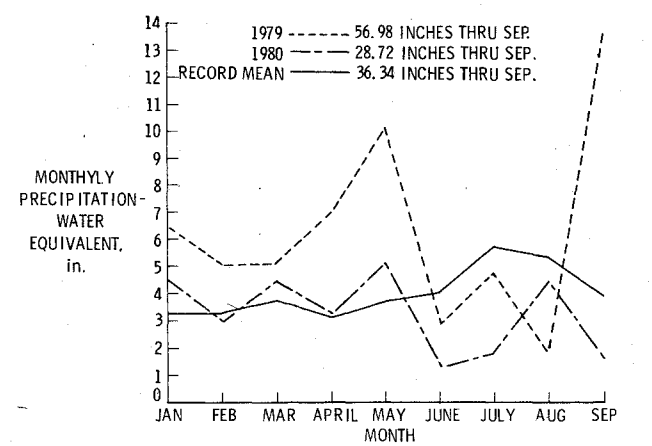

Fig. 7 Average monthly precipitation for the Hampton, Va. area.

measurements, performed on Long Island, N. Y., in 1976 during the initial engineering test of the IHR, indicated a surface level of ~12 ppbv in March 1976 with a decrease to ~0.2 ppbv by July 1976.

The differences between the summer level observed in the Hampton, Va. area and in the Long Island area may be due to climatological conditions or the impact of the more heavily industrialized regions surrounding Long Island. As noted by Levine et al.[8] and discussed below, these "enhanced" levels of ammonia could be the results of rapid volatilization of ammonium nitrate fertilizer applied to agricultural fields several weeks prior to the beginning of our measurements. That the same seasonal trend has been independently observed at two different East Coast locations suggests that this is an annual perturbation on a lower more constant (e.g., for a given season) background level of ammonia. If this is indeed the case, our measurements also suggest that the magnitude of this perturbation, as well as the seasonal background concentration of ammonia, may be strongly dependent upon climatological conditions. Note, for example, the in situ data for the 1980 February to March time period (Fig. 5). The levels of ammonia, while clearly showing an increase over the November to January values, do not reach the same values observed in March 1979 (Fig. 4) or in March 1976.[19] Measurements with the IHR during this same time period also indicated ground level ammonia concentrations on the order of 1 ppbv. Moreover, the background ammonia concentration observed during the summer time period in 1980 was significantly lower than during the previous summer and was, for the most part, below the sensitivity limits of the IHR (e.g., see the far left shaded area in Fig. 4).

Figure 6 illustrates the differences in the ground level ammonia concentrations obtained from in situ measurements at Langley Research Center in 1979 and 1980. It is interesting

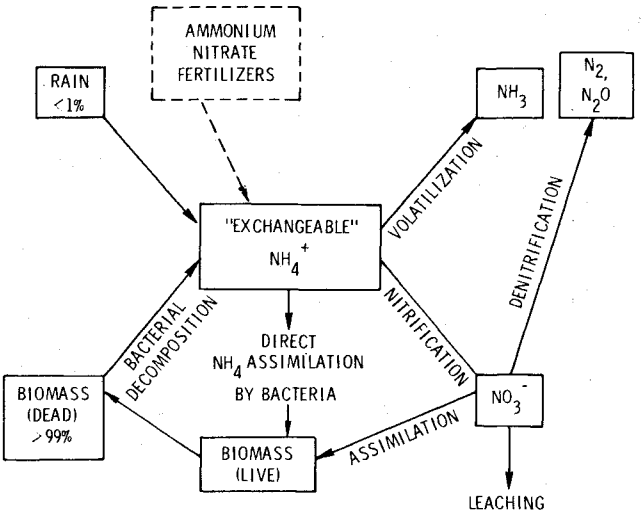

Fig. 8 Ammonia budget of the atmosphere/biosphere system.

to note that in situ measurements of ammonia obtained at Research Triangle Park, N. C., during July and August 1978 by McClenny and Bennett[21] showed ammonia concentrations in the 1.5-5 ppbv range in the absence of rain, while measurements at the same location during July 1980[26] showed ammonia concentrations similar to those observed at the Langley site in the August to September 1980 time frame.

Analysis by Dawson[1] shows that ammonia emission from soil is a strong function of both soil temperature and the soil volume/moisture ratio. The temperature dependence may account, in part, for the seasonal variability observed. However, the relatively high values noted in February 1980 are unexpected, based solely on temperature considerations. Figure 7 shows the monthly precipitation in inches of water for the Hampton, Va. area from January through September for 1979 and 1980 along with the record mean for the past 40 years. In 1979 the total precipitation through September was approximately 57% above the record mean, while in 1980 through September the total precipitation was 21% below the record mean. Even though no direct measurements of soil moisture are available for the area surrounding the Langley sampling site, the precipitation data provide a relative indication of the moisture available in 1979 and 1980. Soil moisture plays an important role in the biological production of ammonia as well as aiding in the release of ammonia via a pumping action during evaporation.[27] The lower ammonia levels we have observed (and those observed by McClenny) throughout 1980 may be a direct consequence of lower soil moisture resulting from less than average rain fall in the Hampton area in particular and the entire Southeast in general.

The Source and Photochemistry of Ammonia

We believe that the enhanced surface levels of NH_3 (10 ppbv) that we measured in March 1979 resulted from the rapid volatilization of ammonium nitrate fertilizer applied to agricultural fields several weeks prior to the beginning of the measurement program. Within two months after the initiation of the measurement program, the surface levels of NH_3 returned to what we assume to be local background levels. A model to quantitatively explain the emission of NH_3 from uncultivated (nonfertilized) soil to the atmosphere has been developed by Dawson.[1] In Dawson's model, "exchangeable" NH_4^+ is supplied to the soil primarily by bacterial decomposition of the biomass, with trace amounts (~1%) supplied by precipitation and dry deposition. Once in the soil, the NH_4^+ can undergo nitrification, forming NO_3^- which can either be assimilated into the biomass or be denitrified, forming gaseous N_2 and N_2O which are returned to the atmosphere. The other route for the NH_4^+ in the soil is the

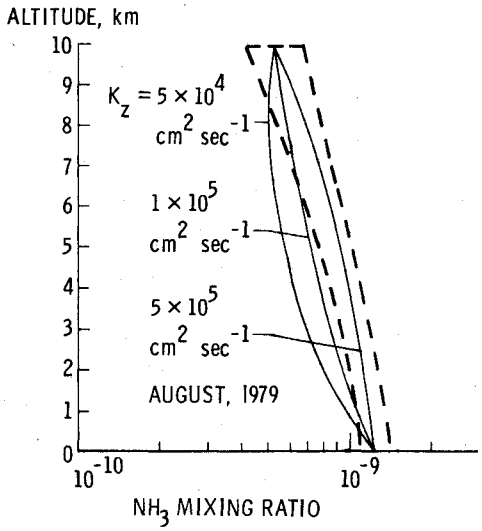

Fig. 9 Effect of the vertical eddy diffusion coefficient, K_z ($cm^2 \cdot s^{-1}$), on the distribution of tropospheric ammonia (typical August 1979 profile is indicated by broken line envelope).

formation of gaseous NH_3 via volatilization which depends on the soil moisture, type, pH, and temperature.[28] Agricultural nitrogen fertilizer, e.g., ammonium nitrate, is an additional source of "exchangeable" NH_4^+ (see Fig. 8). Under optimum volatilization conditions, more than 50% of the "exchangeable" soil NH_4^+ can form gaseous NH_3 (although such a high value would be atypical for efficient agricultural practice).[1] The production of NH_3 via volatilization is rapid, occurring within several weeks of the application of nitrogen fertilizer.[29] Hence, we attribute the high surface levels of NH_3 measured in late March 1979 to the volatilization of NH_4^+ supplied by the application of ammonium nitrate fertilizer to the agricultural fields.

After the period of rapid volatilization (covering our measurement period from late March through early April 1979), simultaneous IHR and ground-based and aircraft in situ NH_3 measurements[20] indicated that the level of 1 ppbv was reached by the beginning of June. From June until August the surface level did not significantly change. During this time period, the measured vertical profiles of NH_3 were characteristic of the typical profile envelope shown in Fig. 9 (e.g., the dashed curve). Consequently, to gain some insight into the atmospheric processes that control the vertical distribution of NH_3 through the troposphere, we assume that the August measurements are typical of the steady-state local troposphere background profile. Numerical simulations of the August measurements were performed using a steady-state tropospheric photochemical model that includes 29 atmospheric gases grouped into the following species families: oxygen species [O_3, O, and $O(^1D)$], nitrogen species (NO, NO_2, HNO_3, HNO_2, NO_3, and N_2O_5), ammonia species (NH_3, N_2H_2, N_2H_3, N_2H_4, NH, and NH_2), carbon species (CH_3OOH, H_2CO, CH_3O, CH_3O_2, HCO, and CH_3), and hydrogen species (H_2O_2, H, OH, and HO_2). Profiles for H_2O, H_2, CO, and CH_4 are specified as input parameters. The model includes 75 photochemical and chemical reactions. The vertical profiles of long-lived tropospheric gases [O_3, $NO_x(NO+NO_2)$, HNO_3, NH_3, N_2H_2, N_2H_3, N_2H_4, CH_3OOH, and H_2O_2] are calculated between the surface and the tropopause (10 km) by the simultaneous solution of the species continuity and flux equations. The species continuity equation is expressed as

$$\partial\phi_i/\partial z = P_i - L_i f_i M \tag{4}$$

where ϕ_i is the flux of the ith species, represented by the flux equation

$$\phi_i = -K_z M(\partial f_i/\partial z) \tag{5}$$

f_i is the species mixing ratio defined as

$$f_i = n_i/M \tag{6}$$

The other terms in these equations are: P_i = the chemical production terms for the ith species; L_i = the chemical loss terms of the ith species; M = the total number density of the atmosphere; and K_z = the eddy diffusion profile in the troposphere.

For chemically short-lived species [O, $O(^1D)$, HNO_2, NO_3, N_2O_5, NH, NH_2, H_2CO, CH_3O, CH_3O_2, HCO, CH_3, H, OH, and HO_2], we can assume photochemical equilibrium and thus the species continuity equation becomes

$$P_i - L_i f_i M = 0 \tag{7}$$

or

$$f_i = P_i/L_i M \tag{8}$$

In our calculations, we have included the following homogeneous (gas to gas) reactions for NH_3 [the loss of NH_3 due to photodissociation ($\lambda \leq 230$ nm) important in the stratosphere is negligible in the troposphere] (reaction rates taken from Hampson and Garvin[30] are in units of $cm^3 s^{-1}$:

$$NH_3 + OH \rightarrow NH_2 + H_2O; \quad K = 2.3 \times 10^{-12} \exp(-800/T) \tag{9}$$

$$NH_3 + O \rightarrow NH_2 + OH; \quad K = 6.6 \times 10^{-12} \exp(-3300/T) \tag{10}$$

$$NH_3 + O(^1D) \rightarrow NH_2 + OH; \quad K = 2.5 \times 10^{-10} \tag{11}$$

The homogeneous loss of NH_3 was found to be controlled by Eq. (9), with Eqs. (10) and (11) resulting in a negligible loss of NH_3. Our calculated OH profile decreases from 2×10^6 cm^{-3} at the surface to 1×10^6 cm^{-3} at 10 km. For this OH profile, the characteristic time for homogeneous loss due to OH varied from about 40 days at the surface to about 180 days at 10 km. The major source of OH in the troposphere is the reaction between $O(^1D)$ and H_2O via

$$O(^1D) + H_2O \rightarrow 2OH; \quad K = 2.3 \times 10^{-10} \tag{12}$$

To test the sensitivity of the calculated NH_3 profile to the OH profile, calculations were performed for a standard H_2O vapor profile at 30° N[31] from the U. S. Standard Atmosphere Supplements, and for profiles of one-half and two times the standard H_2O profile. The resulting changes in both the OH and NH_3 profiles were negligible. The heterogeneous loss term (gas to solid loss) represented by k^* includes the loss of NH_3 due to rainout and dry deposition. The exact details of heterogeneous loss of NH_3 are not known and, hence, all heterogeneous losses are modeled by a single characteristic loss term k^*, which is assumed to be constant from the surface to 5 km and to decrease by a factor of 3 for each kilometer above 5 km. The heterogeneous loss term k^* is related to the characteristic time constant for heterogeneous loss τ^* by $k^* = 1/\tau^*$. Model calculations were made with values of k^* corresponding to values of τ^* ranging 1-150 days to determine the sensitivity of the NH_3 profile to the choice of k^*. The steady-state continuity equation was solved for the NH_3 mixing ratio subject to the lower ($z = 0$ km) and upper ($z = 10$ km) boundary mixing ratios based on the August IHR NH_3 profile shown in Fig. 9, which was assumed to represent the steady-state local tropospheric background of NH_3.

The effect of K_z on the calculated NH_3 profile is shown in Fig. 9. NH_3 profiles have been calculated for values of $K_z = 0.5 \times 10^5$, 1×10^5, and 5×10^5 $cm^2 \cdot s^{-1}$. These calculations were performed for k^* corresponding to $\tau^* = 150$ days. Comparison of our calculations with the measurements indicates a K_z value in excess of 2×10^5 $cm^2 \cdot s^{-1}$, with a best fit for a value of K_z of 5×10^5 $cm^2 \cdot s^{-1}$. The imposed upper

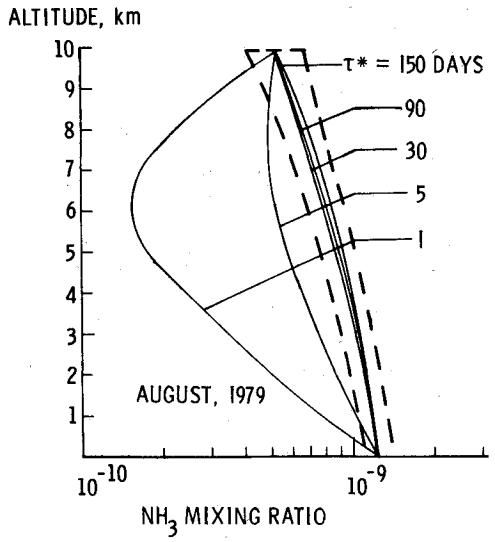

Fig. 10 Effect of the characteristic time constant for heterogeneous loss, τ^* (day), on the distribution of tropospheric ammonia (typical August 1979 profile is indicated by broken line envelope).

boundary conditions unrealistically turns the NH_3 profile back into the measurement envelope for values of K_z less than 2×10^5 cm$^2\cdot$s^{-1} (this numerical artifact incorrectly suggests the existence of an upper tropospheric source of NH_3). A K_z value of 2×10^5 cm$^2\cdot$s^{-1} corresponds to a characteristic transport time of about 35 days, while a K_z of 5×10^5 cm$^2\cdot$s^{-1} corresponds to a transport time of about 15 days. It should be kept in mind, however, that the IHR NH_3 measurements may be biased since they are obtained only on clear, sunny days. Increased solar insolation and heating on such days will lead to increased local convective activity, particularly during the spring and summer when our measurements were obtained.

The effect of τ^* on the calculated NH_3 profile is shown in Fig. 10. Again, the imposed upper boundary condition unrealistically turns the NH_3 profile back into the measurement envelope. These calculations were performed for $K_z=5\times10^5$ cm$^2\cdot$s^{-1}. The best fit is for a τ^* in excess of 10 days, with the lower values of τ^* resulting in profiles significantly below the NH_3 measurement below 6 km. These best fit τ^* values may also be related to the biasing in the IHR measurements. Since the measurements are obtained on clear days, we are selectively eliminating from our data base periods of precipitation, cloudiness, and poor visibility—all periods of possible enhanced heterogeneous loss.

Conclusion

Ammonia is an important tropospheric gas which plays a large role in the photochemistry of the troposphere. It affects the acidity of rain and snow, readily forms ammonium aerosols, and controls the conversion of gaseous SO_2 to sulfate aerosols. Ammonia may affect climate due to its strong absorption around 10 μm, the middle of the atmospheric window. Ammonia has also been suggested as a significant source of stratospheric nitrogen oxides (NO_x), which control levels of ozone in the stratosphere.

We are just beginning to understand the physical, chemical, and biological processes that control the levels of ammonia in the troposphere. The measurements and interpretations presented in this paper suggest that an anthropogenic activity, i.e., the application of ammonium nitrate fertilizer, may have a major impact on the local ammonia budget. Our measurements also suggest that the magnitude of this impact, as well as the seasonal background concentration of ammonia, is strongly dependent upon the climatological parameters which affect soil conditions. Further research in this area is clearly indicated.

Acknowledgments

The authors wish to express their appreciation to William McClenny of EPA, Research Triangle Park, N. C., for providing the photoacoustic cell and Teflon collection tubes and to Robert Braman of the University of South Florida, Tampa, for providing the tungsten oxide coated collection tubes. The authors are also indebted to B. S. Williams and J. A. Williams of NASA Langley Research Center, Hampton, Va. for their skillfull technical assistance.

References

[1] Dawson, G. A., "Atmospheric Ammonia from Undisturbed Land," *Journal of Geophysical Research,* Vol. 82, July 1977, pp. 3125-3133.

[2] Levine, J. S. and Schryer, D. R. (eds.), *Man's Impact on the Troposphere: Lectures in Tropospheric Chemistry,* NASA Ref. Pub. 1022, 1978.

[3] Lau, N-C. and Charlson, R. J., "On the Discrepancy Between Background Atmospheric Ammonia Gas Measurements and the Existence of Acid Sulfates as a Dominant Atmospheric Aerosol," *Atmospheric Environment,* Vol. 11, No. 5, 1977, pp. 475-478.

[4] Wang, W. C., Yung, Y. L., Lacis, A. A., Mo, T., and Hansen, J. E., "Greenhouse Effects Due to Man-Made Peturbations of Trace Gases," *Science,* Vol. 194, Nov. 1976, pp. 685-690.

[5] McConnell, J. C., "Atmospheric Ammonia," *Journal of Geophysical Research,* Vol. 78, Nov. 1973, pp. 7812-7821.

[6] Healy, T. V., McKay, H. A. C., Pilbeam, A., and Scargill, D., "Ammonia and Ammonium Sulfate in the Troposphere over the United Kingdom," *Journal of Geophysical Research,* Vol. 75, April 1970, pp. 2317-2321.

[7] Hoell, J. M., Harward, C. N., and Williams, B. S., "Remote Infrared Heterodyne Radiometer Measurements of Atmospheric Ammonia Profiles," *Geophysical Research Letters,"* Vol. 7, May 1980, pp. 313-316.

[8] Levine, J. S., Augustsson, T. R., and Hoell, J. M., "The Vertical Distribution of Tropospheric Ammonia," *Geophysical Research Letters,* Vol. 7, May 1980, pp. 317-320.

[9] Lovelock, J. E. and Margulis, L., "Atmospheric Homeostasis by and for the Biosphere: The Gaia Hypothesis," *Tellus,* Vol. 26, No. 1-2, 1974, pp. 2-10.

[10] Eriksson, E., "Composition of Atmospheric Precipitation, I, Nitrogen Compounds," *Tellus,* Vol. 4, 1952, pp. 215-232.

[11] Antizzo, J. (ed.), *Health and Environmental Effects of Coal Gasification and Liquefaction Technologies,* Mitre Corp., M78-58, 1978.

[12] Georgii, H. W. and Muller, W. J., "On the Distribution of Ammonia in the Middle and Lower Troposphere," *Tellus,* Vol. 26, No. 1-2, 1974, pp. 180-184.

[13] Roberts, E. R., Selby, J. E. A., and Biberman, L. M., "Infrared Continuum Absorption by Atmospheric Water Vapor in the 8-12 μm Window," *Applied Optics,* Vol. 15, Sept. 1976, pp. 2085-2120.

[14] Goldman, A., Blatherwick, R. D., Murcray, F. W., Van Allen, J. W., Bradford, C. M., Cook, G. R., and Murcray, D. G., "New Atlas of IR Solar Spectra," University of Denver, Colo., ATM-79-27312, March 1981.

[15] McClatchey, R. A., "AFCRL Atmospheric Absorption Line Parameter Compilation," Air Force Geophysical Laboratory, Hanscom AFB, Mass., Environmental Research Paper 434, Jan. 1973.

[16] Seals, R. K. and Peyton, B. J., "Remote Sensing of Atmospheric Pollutant Gases Using an Infrared Heterodyne Spectrometer," *Proceedings of the International Conference on Environmental Sensing and Assessment,* IEEE Annals 75CH1004-I 10-5, Vol. 1, Sept. 1975, pp. 10-14.

[17] Hillman, J. J., Kostiuk, T., Buhl, D., Faris, J. L., Novaco, J. C., and Mumma, M. J., "Precision Measurements of NH_3 Spectral Lines Near 11 μm Using the Infrared Heterodyne Technique," *Optics Letters,* Vol. 1, Sept. 1977, pp. 81-83.

[18] Taylor, F. W., "Spectral Data for the ν_2 Band of Ammonia with Application of Radiative Transfer in the Atmosphere of Jupiter," *Journal of Quantitative Spectroscopy and Radiative Transfer,* Vol. 13, Nov. 1973, pp. 1181-1217.

[19] Peyton, B. J., Lange, R. A., Savage, M. G., Seals, R. K., and Allario, F. A., "Infrared Heterodyne Spectrometer Measurements of Vertical Profiles of Tropospheric Ammonia and Ozone," AIAA Paper 77-73, Jan. 1977.

[20] Hoell, J. M., Harward, C. N., and McClenny, W. A., "Comparison of Remote Infrared Heterodyne Radiometer and In Situ Measurements of Atmospheric Ammonia," Paper presented at Conference on Laser and Electro-Optical Systems, San Diego, Calif., Feb. 1980.

[21] McClenny, W. A. and Bennett, C. A. Jr., "Integrative Technique for Detection of Atmospheric Ammonia," *Atmospheric Environment,* Vol. 14, No. 6, 1980, pp. 641-645.

[22] Braman, R. S., Shelley, T. J., and McClenny, W. A., "Tungstic Acid for Preconcentration and Determination of Gaseous and Particulate Ammonia and Nitric Acid in Ambient Air," accepted for publication in *Analytic Chemistry*, Jan. 1982.

[23] Harward, C. N., McClenny, W. A., Hoell, J. M., Williams, J. A., and Williams, B. S., "Ambient Ammonia Measurements in Coastal Southeastern Virginia," accepted for publication in *Atmospheric Environment.*

[24] McClenny, W. A., Bennett, C. A., Russwurm, G. M., and Richmond, R., "Optoacoustic Cell Design for Trace Gas Analysis Using a Helmholtz Resonator," *Applied Optics*, Vol. 20, Feb. 15, 1981, pp. 650-653.

[25] Baumgardner, R. E., McClenny, W. A., and Stevens, R. K., "Optimized Chemiluminescence System for Measuring Atmospheric Ammonia," Environmental Protection Agency, Pub. 600/2-79-028, 1979.

[26] McClenny, W. A., Private communication, Environmental Protection Agency, RTI, NC, 1980.

[27] Bartholomew, W. V. and Clark, F. E. (eds.), *Soil Nitrogen,* Agronomy Series, No. 10, American Society of Agronomy, 1965.

[28] Fenn, L. B. and Escarzaga, R., "Ammonia Volatilization from Surface Applications of Ammonium Compounds on Calcareous Soils, V. Soil Water Content and Methods of Nitrogen Application," *Journal of Soil Science Society of America,* Vol. 40, No. 4, 1976, pp. 536-541.

[29] Dawson, G. A., Private communication, Institute of Atmospheric Physics, University of Arizona, Tucson, Arizona, 1979.

[30] Hampson, R. G. and Garvin, D., *Reaction Rate and Photochemical Data for Atmospheric Chemistry,* NBS Special Publication 5B, 1977.

[31] *U. S. Standard Atmosphere Supplements,* U. S. Government Printing Office, Washington, D. C., 1966.